Simulation, Prediction, and Verification of the Corrosion Behavior of Cu-Ag Composite Sintered Paste for Power Semiconductor Die-attach Applications

Wang, Xinyue; Yang, Zhoudong; Zhang, Guoqi; Zhang, Jing; Liu, Pan

DOI
10.1109/ECTC51909.2023.00341

Publication date
2023

Document Version
Final published version

Published in
Proceedings - IEEE 73rd Electronic Components and Technology Conference, ECTC 2023

Simulation, Prediction, and Verification of the Corrosion Behavior of Cu-Ag Composite Sintered Paste for Power Semiconductor Die-attach Applications

Xinyue Wang
Academy for Engineering and Technology, Fudan University
Shanghai, China
22110860005@m.fudan.edu.cn
(First Author)

Zhoudong Yang
Laboratory of Advanced Materials, Fudan University
Shanghai, China
20213010003@fudan.edu.cn

Guoqi Zhang
Electronic Components, Technology, and Materials, Delft University of Technology
Delft, the Netherlands
g.q.zhang@tudelft.nl

Jing Zhang
Heraeus Materials Technology Shanghai Ltd.
Shanghai, China
j.zhang@heraeus.com

Pan Liu
[1]*Academy for Engineering and Technology, Fudan University;* Shanghai, China
[2]*Research Institute of Fudan University in Ningbo*; Ningbo, China
panliu@fudan.edu.cn
(Corresponding Author)

2023 IEEE 73rd Electronic Components and Technology Conference (ECTC) | 979-8-3503-3498-2/23/$31.00 ©2023 IEEE | DOI: 10.1109/ECTC51909.2023.00341

***Abstract*—With the popularization of wide band-gap power modules in offshore wind power systems and water surface photovoltaic power stations, packaging materials face challenges of corrosion by salt, blended with high humidity. Copper-silver (Cu-Ag) composite sintered paste was proposed by researchers as a novel die-attach material for a lower cost and anti-electromigration ability. However, the potential difference between copper and silver forms galvanic corrosion in a high-humidity environment, resulting in accelerated failure combined with salt mist. To further promote the application of composite sintered materials, a copper-silver double-sphere galvanic corrosion model based on finite element simulation was proposed in this paper. The relationship between corrosion rate and time of different Cu-Ag particle size combinations under different sintering degrees was predicted by initial exchange current density. Through the electrochemical characterization of the sintered samples, the optimal combination of materials was further discussed. The accuracy of the model was also verified. The conclusions obtained from both the experiments and simulation work provide guidance for future anti-corrosion analysis, as well as the reliability improvement of novel composite sintered materials.**

Keywords—die-attach material; power electronic packaging; FEM simulation; galvanic corrosion

I. INTRODUCTION

With the increasing application of wide band-gap semiconductor devices in multiple application fields, higher requirements are put forward for the corresponding electronic packaging materials[1-3]. As a representative commercial die-attach material, sintered silver is suitable for high frequency, high temperature, and high power applications[4]. However, silver is prone to electrochemical migration under the harsh service environment of high humidity, which has a negative impact on the reliability of devices, especially for offshore wind power systems and water surface photovoltaic power stations[5, 6]. Hence, novel solutions such as copper-silver(Cu-Ag) composite sintered paste have been introduced[7].

Cu-Ag composite joints, compared to pure silver joints, have similar shear strength, better electromigration resistance, and cheaper cost[8]. However, the potential difference between copper and silver forms galvanic corrosion that leads to rapid failures of devices, especially under high-humidity environments[9]. At present, great efforts have been devoted to improving the shear strength and electrical conductivity of such sintered materials, while the research on electrochemical corrosion has not received enough attention[7, 8]. Hence, an investigation is needed to study the specific electrochemical corrosion process of Cu-Ag composite sintered materials to further improve the overall reliability of power modules, thus promoting practical applications.

In this work, we proposed a galvanic corrosion model to promote the electrochemical corrosion research of Cu-Ag composite sintered materials. The model is a double-sphere model established by finite element simulation in COMSOL Multiphysics 5.6 software. Through the simulation calculation of different copper-silver particle size groups in sodium chloride solution (simulated seawater), the relationship between corrosion rate and time of copper-silver, in combination with different densification degrees, was investigated. Then, three kinds of Cu-Ag particle size combinations were prepared by the pressureless sintering process. The model was verified by the experimental data of electrochemical tests of samples immersed in sodium chloride (NaCl) solution for 28 days. At the same time, combining the test results with the Arrhenius formula, the explanation, and verification of the corrosion rate difference on kinetic were further explored. Such work was intended to

2377-5726/23/$31.00 ©2023 IEEE
DOI 10.1109/ECTC51909.2023.00341

accelerate the development of new composite sintered materials and provide a theoretical basis and guidance for the selection of raw material particle size of high-reliable Cu-Ag composite sintered materials.

II. Simulation Model Description

The relationship between the sintering degree and particle size combination of copper-silver blend particles and the corrosion rate was set and calculated by the finite element method. During the sintering process, the two metal particles start to contact and then form a sintering neck. Due to the different particle size matching and densification degrees, the potential difference of copper-silver contact formation and the distribution of surface electric field and current density are different. Therefore, the tolerance to corrosion also varies. To study the effect of different contact conditions on the corrosion rate of Cu-Ag composite sintered materials, a double-sphere model was first established to simulate the contact of two metals after sintering. Then, the corrosion module in COMSOL Multiphysics 5.6 software was applied. The open circuit voltage and exchange current density data measured in sodium chloride solution of copper and silver sintered materials were introduced respectively to establish the initial electric field distribution and current density vector distribution. Finally, the variation of the maximum corrosion rate of the material with time during the 10-day corrosion process was further derived.

The geometric design of the sintering system and meshing are shown in Figure 1, with the main parameters of the model shown in Table 1. In the simulation, the right side was set as a copper particle with a fixed diameter of 500 nm. The left side was set to be a silver particle with a diameter of 300 nm, 500 nm, and 800 nm respectively, to simulate the contact of different particle sizes, as shown in Figure 2. In the simulation work, in order to pay attention to the influence of particle size combination and contact degree between particles on the corrosion rate, the plastic deformation around the sintering neck was ignored.

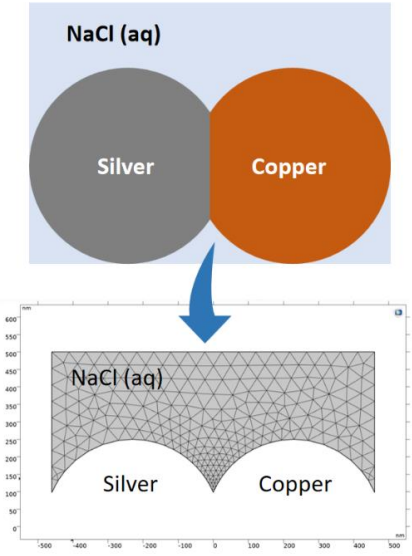

Figure 1. Schematic of the geometrical model.

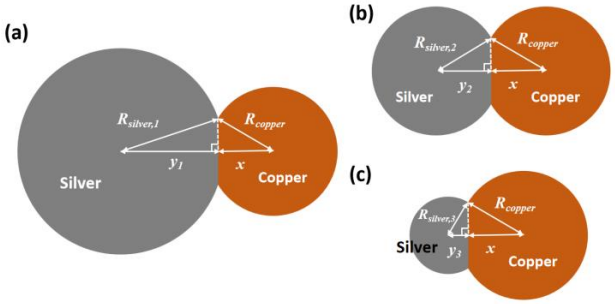

Figure 2. The schematic diagram of the sintering connection of different Cu-Ag particle size combinations: the model of (a) $R_{silver,1}>R_{copper}$; (b) $R_{silver,2}=R_{copper}$; (c) $R_{silver,3}<R_{copper}$.

TABLE I. The Main Parameters of The Model

Parameter	*Value*
R_{copper}	250 nm
$R_{silver,1}$	400 nm
$R_{silver,2}$	250 nm
$R_{silver,3}$	150 nm
Electrical conductivity of NaCl solution	5 S/m

The difference in sintering degree was simulated by adjusting the distance between the two particle centers. The radius of the two spheres was R_{copper} and R_{silver}, respectively, where the value of R_{copper} was fixed. The distance from the center of the copper and silver particles to the contact surface was x and y, respectively. The diameter of the sintering neck was $2d$, and its geometric relationship can be expressed as Equation (1).

$$d^2 = R_{silver}^2 - y^2 = R_{copper}^2 - x^2 \tag{1}$$

Since the size of the copper particle size was fixed, the value of x/R_{copper} was applied to uniformly represent the degree of sintering. In addition, y can be expressed as:

$$y = \sqrt{R_{silver}^2 - \left(R_{copper}^2 - x^2\right)} \tag{2}$$

Equation (2) was utilized for geometric position calculation when R_{silver} was determined in the corresponding modeling process.

III. Simulation Results

A. Comparison of different degrees of sintering (x/R_{copper})

Different sintering processes (temperature, pressure, time) lead to different degrees of sintering connection. Therefore, different x/R_{copper} values (0.94, 0.92, 0.90, 0.88) were set to describe the sintering neck formed by different sintering degrees in the simulation. The smaller the value of x/R_{copper}, the better the degree of densification of sintering.

Figure 3 exhibited the results of the relationship between maximum corrosion rate and time (<10 days) of three groups of Cu-Ag sintered bodies with different particle size combinations. The results showed that when the diameter of the silver particle was 800 nm (Fig. 3(a)), the initial maximum corrosion rate was about 10 nm/day, and the corrosion rate grew slightly with the decline of the x/R_{copper} value. In addition, the prediction results of different densification degrees illustrated that the corrosion rate showed a significant upward trend with the immersion time. When the diameter of the silver particle was consistent with that of copper (Fig. 3(b)), the initial maximum corrosion rate was 5.76 nm/day, which was independent of the x/R_{copper} value. However, with the corrosion time prolonged, the sample group with higher sintering densification showed a relatively faster corrosion rate. Interestingly, when the silver particle size was smaller than copper (300 nm), as shown in Figure 3(c), the initial maximum corrosion rate dropped to about 2.3 nm/day. The corrosion rate decreased with the rose of the densification degree. Meanwhile, the growth rate of the maximum corrosion rate was almost consistent over time.

B. Comparison of different particle size combinations

According to the simulation results in the previous section, the influence of different sintering degrees on the maximum corrosion rate was less than that caused by particle size change. Hence, to further explore the reasons for the maximum corrosion

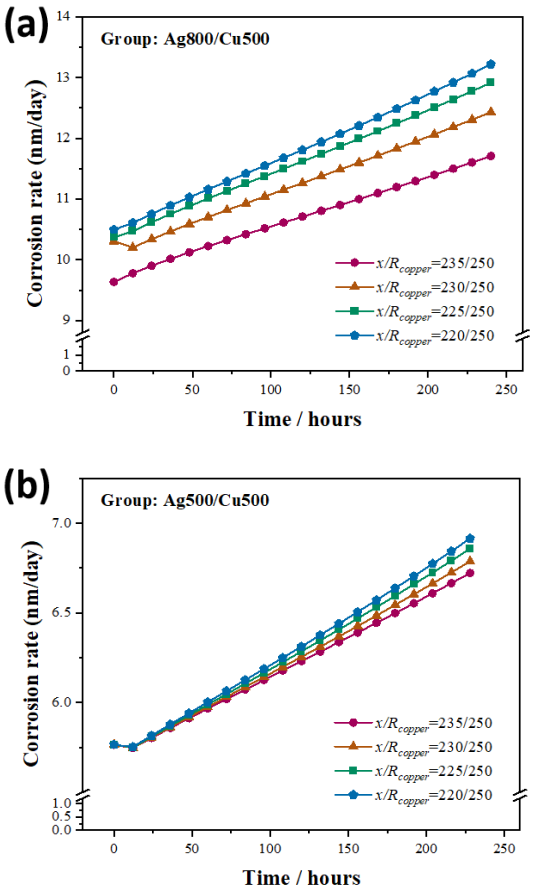

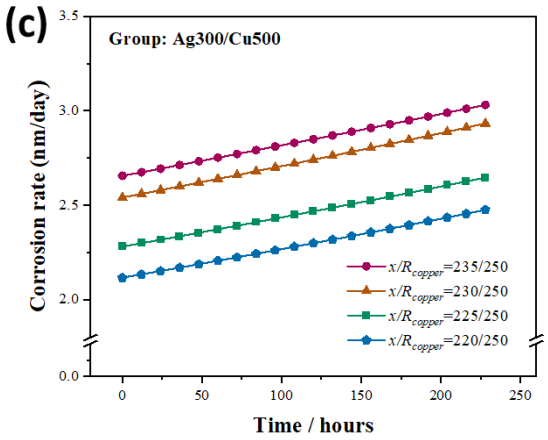

Figure 3. The results of the relationship between maximum corrosion rate and time: (a) $R_{silver,1}$=400 nm; (b) $R_{silver,2}$=250 nm; (c) $R_{silver,3}$=150 nm.

rate changes over time brought by different particle size combinations, we fixed the sintering degree (x/R_{copper}) as 0.92 and obtained the simulation results of the electrolyte potential and current density vector distribution of the three groups of particle size combinations at initial and after 10 days of corrosion, as shown in Figure 4.

With the decrease in silver particle size, the corrosion degree of copper on the right declined gradually. The potential difference and current density on the surface were more concentrated on smaller particles. Therefore, the smaller the copper particles are relative to the silver particles, the greater the change in the electric potential on the surface of the copper particles and the greater the current density, leading to the intensification of corrosion. It is worth mentioning that the corrosion degree of Cu-Ag contact in group Ag300/Cu500 was slighter compared to group Ag800/Cu500 and Ag500/Cu500. According to the potential distribution diagram, it was speculated that the relative potential of the sintered neck near the contact position was the lowest. Hence, with the shrinkage of silver particle size, the copper near the surface of the Cu-Ag sintered neck exhibited anti-corrosion behavior due to the ability of fewer electrons lost.

Overall, the difference in corrosion rate was caused by the discrepancy in the potential distribution and current density formed after the two particles come into contact. This conclusion also explained the change in corrosion rate caused by different sintering degrees (The phenomena in Figure 3): The current lines mainly concentrated on the surface of smaller particles, and with the increase of sintering degree, the current density value was further enhanced. Since the smaller initial particle size of silver particles in Ag300/Cu500 compared to copper, the initial current density was concentrated on the surface of silver rather than copper. Therefore, the corrosion rate of copper showed a completely opposite trend with the change of densification degree, compared with Ag800/Cu500 and Ag500/Cu500 samples.

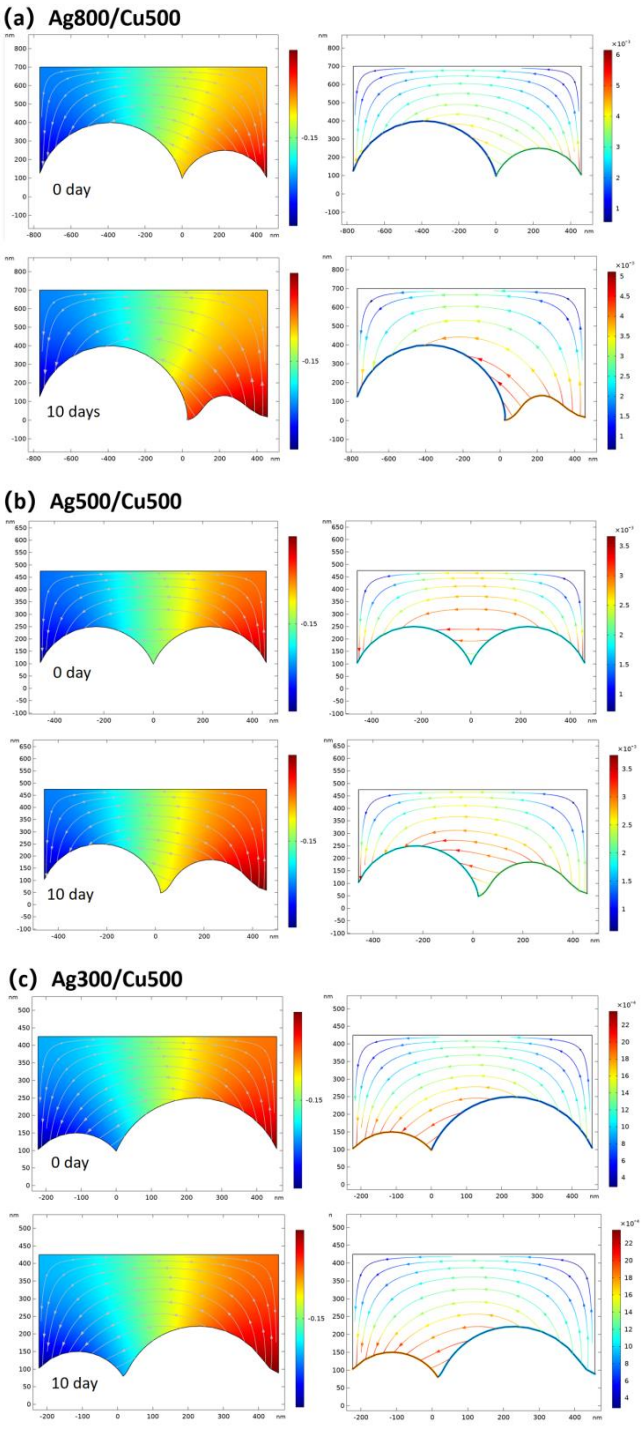

Figure 4. The simulation results of the electrolyte potential (left column / V) and current density vector distribution (right column / A•m^{-2}) of the three groups of particle size combinations at initial and after 10 days of corrosion: (a) $R_{silver,1}$=400 nm; (b) $R_{silver,2}$=250 nm; (c) $R_{silver,3}$=150 nm.

IV. Validation

To verify the above simulation results, three groups of copper-silver composite sintering pastes were configured corresponding to the simulation parameter settings. The sintered samples were first prepared under a pressure-less sintering process, then immersed in imitated seawater environment for 28 days for actual corrosion tests. Finally, the sample characterization test data were analyzed to further discuss the accuracy of the model and the mechanism of corrosion reaction. The detailed experimental verification process was as follows:

A. Materials and samples

Commercialized copper powder (mean diameter 500 nm) and silver powders (mean diameter 800nm, 500nm, and 300nm, respectively) were selected for the preparation of Cu-Ag composite sintered pastes, as shown in Figure 5.

Each paste consists of silver powder (43wt%), copper powder (43wt%), and solvent (14wt%). The solvent included polyethylene glycol and terpineol. After homogenization, the sintered samples were fabricated through stencil printing and pressure-less sintering in the oven, as shown in Figure 6. The sintering temperature was 250℃ and the time was 90 minutes. Flexible polyimide (PI, thickness 0.15mm) was selected as the substrate to facilitate the stripping of the sintered samples.

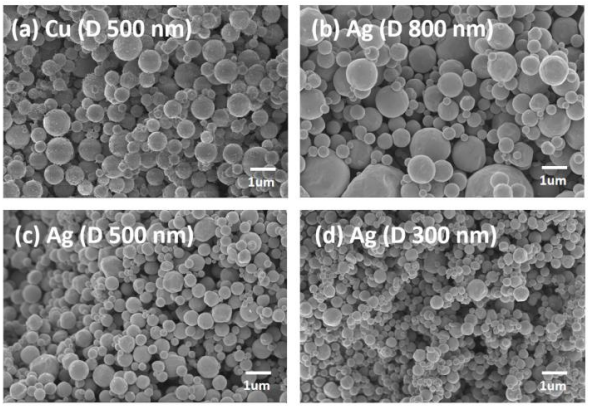

Figure 5. SEM photos of copper and silver particles: (a) Copper powder with an average diameter of 500 nm; Silver powder with average diameters of (b) 800 nm, (c) 500 nm, and (d) 300 nm.

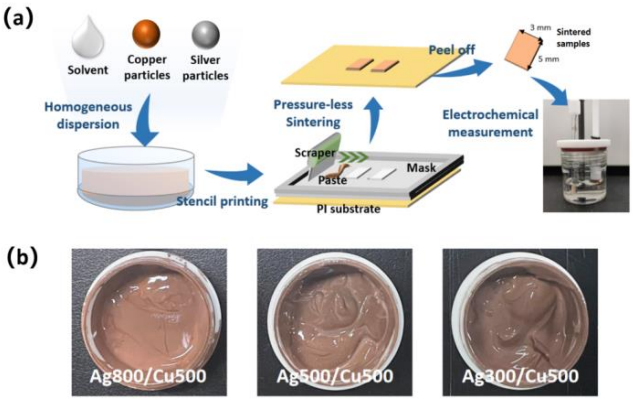

Figure 6. (a) Schematic diagram of sample preparation; (b) Photos of the prepared pastes

The scanning electron microscope (SEM, Zeiss) photos of sintered samples were presented in Figure 7, which proved the contact between Cu-Ag particles in each group of samples after sintering.

After preparing the sintered samples, three groups of composite sintered materials were immersed in 3.5wt% NaCl solution to simulate corrosion in a seawater environment. To observe significant corrosion differences, the samples were etched at room temperature for a total of 28 days. X-Ray Diffraction (XRD, BRUKER) using Cu K_α radiation (λ=0.15418 nm) was utilized to characterize the corrosion products. The results were shown in Figure 8, indicating that the main corrosion products were copper oxides. The phases of silver oxide and silver chloride were not found, indicating that copper corrodes first in NaCl solution when Cu and Ag were in contact.

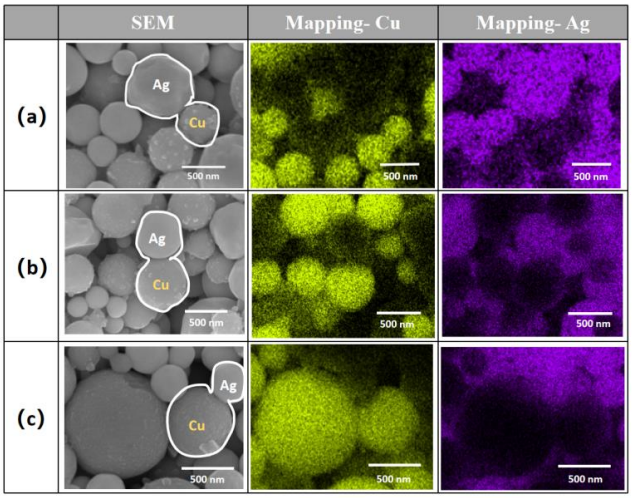

Figure 7. SEM photos of sintered samples before corrosion: (a) Ag800/Cu500; (b) Ag500/Cu500; (c) Ag300/Cu500.

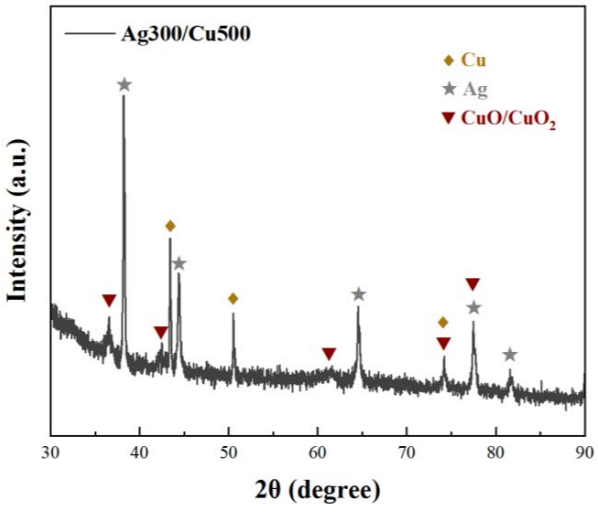

Figure 8. The result of XRD of sample Ag300/Cu500 after soaking in NaCl solution for 28 days

B. *Electrochemical measurement*

To characterize the changes of samples before and after immersing in 3.5wt% NaCl solution for 4 weeks, polarization curve measurements and electrochemical impedance spectroscopy (EIS) were operated on the EC-Lab electrochemical workstation (Biologic VSP-3e). The polarization curves were tested from -0.4 V to 0.3 V (vs. SSCE), under a scan rate of 120 mV/min. The frequency range of the EIS test was scanned from 10^{-1} to 10^5 Hz with a disturbance amplitude of 5 mV.

a) *Polarization curve measurements:* Figure 9 displayed the polarization curves of the sintered samples in NaCl solution before and after being exposed for 28 days. The corresponding values calculated from the polarization curves are listed in Table 2, including anodic and cathodic Tafel slope (βa and βc), corrosion potentials (E_{corr}), and corrosion current densities (I_{corr}). It is obliviously that the E_{corr} of the three samples at initial states were almost identical, while the I_{corr} increased with the increase of the diameter of silver in the sintered body, which was exactly consistent with the trend of potential distribution and current density in the simulation results. After 4 weeks, the E_{corr} reduction of sample Ag800/Cu500 was much larger than that

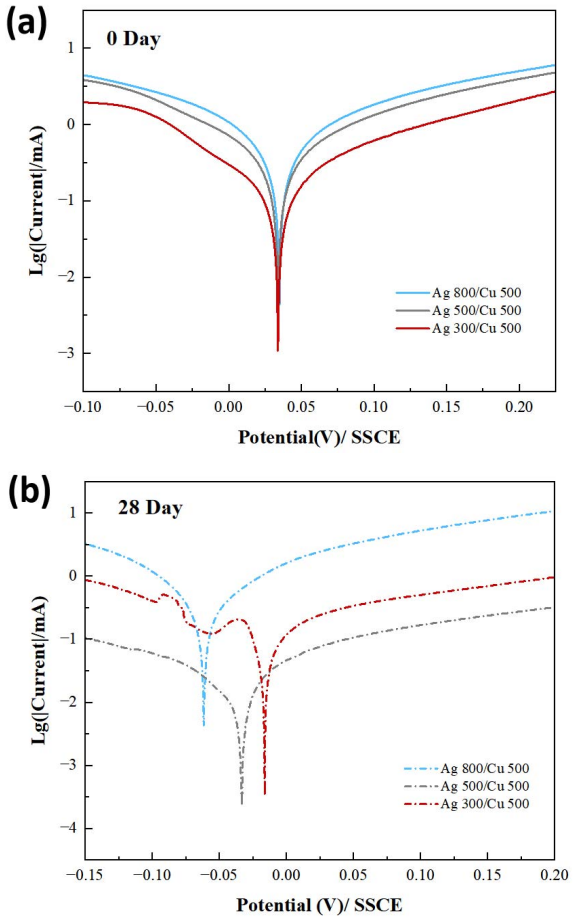

Figure 9. The polarization curves of the sintered samples in NaCl solution before and after corrosion for 28 days

TABLE II. THE CHARACTERISTIC PARAMETERS OBTAINED BY POLARIZATION CURVES IN FIGURE 9.

Samples	Corrosion time (days)	β_a	$I_{corr,a}$ (mA)	β_c	$I_{corr,c}$ (mA)	E_0 (V)	E_{corr} (V)	I_{corr} (mA)
Ag800/Cu500	0	0.073873	0.62783	-0.071251	0.63437	0.035000	0.035376	0.63103
Ag800/Cu500	28	0.066347	0.53234	-0.061018	0.57947	-0.061700	-0.059004	0.55442
Ag500/Cu500	0	0.076994	0.55134	-0.073863	0.54842	0.034100	0.033900	0.54991
Ag500/Cu500	28	0.090394	0.18217	-0.054284	0.11981	-0.033200	-0.04712	0.15567
Ag300/Cu500	0	0.074650	0.38827	-0.087021	0.40193	0.033900	0.035289	0.39556
Ag300/Cu500	28	0.097286	0.36771	-0.053284	0.35824	-0.016200	-0.015302	0.36157

of sample Ag300/Cu500, revealing that the sample with smaller silver particles had a significant advantage in corrosion resistance, corresponding with the predicted trend of the finite element simulation in *Section III*. It is worth mentioning that the I_{corr} showed a downward trend after corrosion, and the I_{corr} of sample Ag500/Cu500 decreased most obviously. We speculated that this phenomenon is due to the accumulation of corrosion products (oxides of copper) with low conductivity on the surface, conducted the decrease of corrosion rate in kinetics.

b) *Variable temperature EIS measurements:* To further illustrate the difference in the corrosion resistance of the three kinds of Cu-Ag composite sintered samples, we studied the EIS curves of the initial samples at a series of temperatures of 303, 313, 323, and 333 K by measuring the energy barrier (E_a). Then based on the Arrhenius equation, the E_a of each sample was obtained by fitting the R_{ct} values, as shown in Figure 10(a). The E_a values of the three samples are given in Figure 10(b). The Ag300/Cu500 sample has the highest E_a value (1.22 eV, compared to 0.62 eV for Ag500/Cu500 and 0.38 eV for Ag800/Cu500), indicating that it has the best corrosion resistance under the same test conditions, which are also consistent with the simulation results.

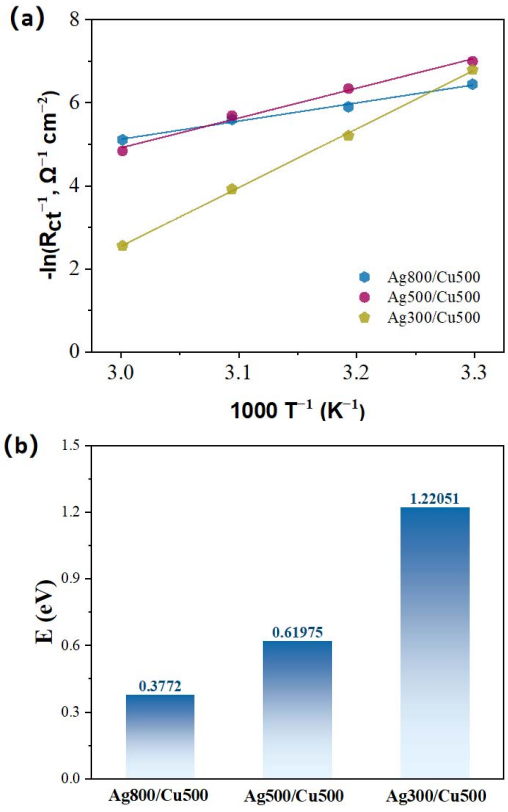

Figure 10. (a) Arrhenius plots of R_{ct} values and (b) the activation energy for 3 kinds of Cu-Ag composite sintered samples.

According to the actual experimental results, the simulation results in this work are in agreement with the initial stage of corrosion, and the prediction of corrosion resistance is also accurate. However, with the extension of time, the deviation still existed in the prediction of corrosion current. Therefore, the simulation model still needs to be further improved, such as considering the influence of corrosion product generated on the surface on the corrosion rate. Further work will be combined with a detailed analysis of corrosion products to optimize the model.

V. CONCLUSIONS

In this work, a two-sphere galvanic corrosion model of Cu-Ag composite sintered materials based on FEM was introduced. Through adjusting the contact degree and particle size combination between the Cu and Ag particles, the maximum corrosion rates of the two particles under different sintering conditions were obtained. Different corrosion rates were analyzed with the simulated potential distribution and the current density vector distribution. The pressureless sintered samples prepared in the laboratory were corroded in 3.5wt% NaCl solution and characterized by SEM, XRD, and electrochemical workstation. The model was verified with the actual measured data.

The results demonstrated that the E_{corr} was consistent for all samples at the beginning. It has been found that the I_{corr} decreased with the decrease of silver particle size at the early stage of corrosion, which agreed with the simulation results. After 4 weeks of exposure to 3.5wt% NaCl solution, the reduction of E_{corr} in accordance with the particle size of silver, indicating that the Ag300/Cu500 combination is more resistant to corrosion in such an environment. It was also consistent with the trend of the simulation results. However, the corrosion current density decreased with the corrosion time. Such a phenomenon was contrary to the trend of the simulations and

was probably caused by the accumulation of corrosion products such as copper oxide on the surface.

In summary, the models based on copper-silver blend particles have potential applications in sintered material analysis for corrosion, which provided information with different degrees of sintering densification. These are of great significance to the development of new products and the improvement of the reliability of power semiconductor packaging.

ACKNOWLEDGMENT

In this work, the authors would like to thank the Research Institute of Fudan University in Ningbo (Ningbo Science & Technology Innovation 2025 Major Project 2022Z089), Shanghai Science & Technology Commission (20501110702), Shanghai SiC Power Devices Engineering & Technology Research Center (19DZ2253400), and Yiwu Research Institute of Fudan University (20-1-03) for funding this research on providing simulation support and laboratory accesses. Many thanks to Heraeus Materials Technology Shanghai Ltd. for prototype validation and Ms. Haixue Chen, a graduate student from Fudan University for characterization support, respectively.

REFERENCES

[1] W. Chi, Y. Huang, H. Chen, P. Chen, C. Chang, and H. Liao, "Silver sintering die attachment for power chip in power module," in 2017 12th International Microsystems, Packaging, Assembly and Circuits Technology Conference (IMPACT): IEEE.

[2] J. N. Chijioke and V. Kiray, "A Review of Power Electronics Applications for Wind Energy Systems in Microgrids," Journal of Scientific Research and Reports, pp. 139-148, 2020.

[3] H. Lee, V. Smet, and R. Tummala, "A Review of SiC Power Module Packaging Technologies: Challenges, Advances, and Emerging Issues," IEEE Journal of Emerging and Selected Topics in Power Electronics, vol. 8, no. 1, pp. 239-255, 2020.

[4] W. Guo, Z. Zeng, X. Zhang, P. Peng, and S. Tang, "Low-Temperature Sintering Bonding Using Silver Nanoparticle Paste for Electronics Packaging," Journal of Nanomaterials, vol. 2015, no. 2, pp. 1-7, 2015.

[5] B. Liao et al., "Electrochemical migration behavior of low-temperature-sintered Ag nanoparticle paste using water-drop method," Journal of Materials Science: Materials in Electronics, vol. 32, no. 5, pp. 5680-5689, 2021.

[6] E. Kolbinger, S. Wagner, A. Gollhardt, O. Rämer, and K. D. Lang, "Corrosion behavior of sintered silver under maritime environmental conditions," Microelectronics Reliability, vol. 88-90, pp. 715-720, 2018.

[7] K. S. Tan, K. Y. J. M. Cheong, and Design, "Mechanical properties of sintered Ag – Cu die-attach nanopaste for application on SiC device," Materials and Design, vol. 64, no. 9, pp. 166-176, 2014.

[8] Y. Morisada, T. Nagaoka, M. Fukusumi, Y. Kashiwagi, M. Yamamoto, and M. Nakamoto, "A Low-Temperature Bonding Process Using Mixed Cu – Ag Nanoparticles," Journal of Electronic Materials, vol. 39, no. 8, pp. 1283-1288, 2010.

[9] H. Huang and F. Bu, "Correlations between the inhibition performances and the inhibitor structures of some azoles on the galvanic corrosion of copper coupled with silver in artificial seawater," Corrosion Science, vol. 165, 2020.